Chakraborty, M., Mukherjee, A., Ahmed, K.M., Fryar, A.E., Bhattacharya, A., Zahid, A., Das, R., and Chattopadhyay, S., 2021, Influence of hydrostratigraphy on the distribution of groundwater arsenic in the transboundary Ganges River aquifer system, India and Bangladesh: GSA Bulletin, https://doi.org/10.1130/B36068.1.

Supplemental Material

Table S1. Details of borehole litholog data used for the lithological model

Table S2. Details of groundwater arsenic data

Figure S1. The depth distribution of the borehole lithologs used for the lithological model.

Figure S2. Distribution of the borehole lithologs in a three-dimensional geospatial framework.

Figure S3. (A) Map showing the spatial distribution of borehole lithologs within the Ganges River delta; (B) Lithologic model of the Ganges River delta subsurface (to a depth of 300 m below MSL). Viewed from northwest and southeast.

Figure S4. Plan view of the spatial disposition of gravel layers within the Ganges River delta subsurface (up to a depth of 300 m below msl).

Figure S5. Model validation (first step), showing 62 test boreholes overlaid on the predicted lithological framework of the Ganges River delta subsurface along 3 sections that passes through these boreholes.

Figure S6. Model validation (second step), showing 25 boreholes [compiled from Umitsu (1987), Goodbred and Kuehl (2000), and Goodbred et al. (2014)] overlaid on the predicted lithological framework of the Ganges River delta subsurface along 3 cross-sections that pass through these boreholes.

Figure S7. Map showing the distribution of groundwater arsenic concentration within the Ganges River delta, developed using kriging.

Figure S8. Kernel density (bandwidth = 0.5) plots showing the distribution of dissolved Fe among the major aquifer sub-systems of the delta.

Figure S9. 2-dimentional modeled lithological sections (to a depth of 300 m below msl) along four north-south and three east-west directions across the Ganges River delta.

Influence of hydrostratigraphy on the distribution of groundwater arsenic in the transboundary Ganges River aquifer system, India and Bangladesh

Madhumita Chakraborty[a], Abhijit Mukherjee[a,b], Kazi Matin Ahmed[c], Alan E. Fryar[d], Animesh Bhattacharya[b], Anwar Zahid[e], Raja Das[f], Siddhartha Chattopadhyay[g]

[a]*Department of Geology and Geophysics, Indian Institute of Technology Kharagpur, Kharagpur, India*

[b]*School of Environmental Science and Engineering, Indian Institute of Technology Kharagpur, Kharagpur, India*

[c]*Department of Geology, University of Dhaka, Dhaka, Bangladesh*

[d]*Department of Earth and Environmental Sciences, University of Kentucky, Kentucky, KY 40506-0053, USA*

[e]*Bangladesh Water Development Board, Green Road, Dhaka 1205, Bangladesh*

[f]*Center for Geospatial Analytics, North Carolina State University, Raleigh, NC 27695, USA*

[g]*Department of Humanities and Social Sciences, Indian Institute of Technology Kharagpur, Kharagpur, India*

Corresponding Author: A. Mukherjee (amukh2@gmail.com; abhijit@gg.iitkgp.ac.in)

Supplementary Methods:

Lithologic Modeling:

The borehole lithologs that were used for the lithologic modeling for this study was complied from various published govormnetal database (refer to SI Table 1 for data sources). These boreholes were constructed mostly for the installation of government drinking water and monitoring wells. The depth of these boreholes ranges up to 450 m below MSL, wherein ~92% of wells exceed 70 m depth below MSL, ~63% of wells exceed 150 m below MSL, and ~14% of wells exceed 300 m depth below MSL (SI Figure 1). The lithologs from these boreholes record detailed, depth-specific descriptions of the delta sediments. Owing to its the multiple sources, the data inherently involved differences in the standards of observation, mainly in the context of the in-field identification of the lithotypes. Thus, for comprehensible representation of the aquifer-aquitard geometry on a regional scale, the detailed lithologic descriptions were grouped into four dominant lithotypes, i.e., gravel, sand, silt, and clay, based on the relative proportion of the sediment classes as understood from the detailed lithologic descriptions. The elevation of each borehole (above MSL) was extracted from the digital elevation model developed by the Shuttle Radar Topography Mission (SRTM 90; Harris Geospatial Solutions) with a horizontal resolution of 90 m and vertical resolution of 1 m. The borehole locations were projected to Universal Transverse Mercator (UTM 1983) (datum WGS 84 1984 [NAD 83], zone 45) in meters. The lithologs were randomly split into 90% for training and 10% for testing of the lithologic model.

For the model development, the entire volume of the model was discretized using block-centric finite-difference grids upto a depth of 300 m below MSL, which is the maximum depth limit of the model. The model sensitivity was iteratively optimized by adjusting the model resolution and the final model was developed with a horizontal resolution of 1 km (x) × 1 km (y) and a vertical resolution of 2 m (z). This resulted in the generation of a total of 18,821,550 nodes [110,715 (xy) ×170 (z nodes)] and a model volume of ~37,643 km^3. The Lateral Blending Lithologic Modeling algorithm was used for the model generation. This method obeys the nearest neighbor algorithm, but with an inherent lateral bias, i.e., for each voxel node, the search is limited to the horizontal directions within the model volume. The model was developed in RockWorks17 (RockWare, Golden, CO, USA).

Hydrostratigraphic classification:

The occurrence of intricately intercalated strata with contrasting hydraulic characteristics can significantly alter the effective hydraulic properties (e.g., effective porosity and permeability) of the aquifer system. Hence, spatial variations in the geometry and distribution of aquitards and the extent of intercalation can result in a distinctly different aquifer system and groundwater flow properties (Michael and Voss, 2009). Based on this hypothesis, the sub-systems were delineated using a knowledge-driven classification approach that involved integrated consideration of the following aspects: (a) the lateral extent of intercalating aquitards, (b) frequency of occurrence of the intercalating aquitards along with depth profile, and (c) thickness of the surficial confining unit. The parameter value ranges for these factors within each aquifer sub-system are elaborated in the results section. However, isolated aquitards having lower spatial extent (~10 km) and/or thickness (~5 m) are expected to have an inconsequential impact as confining units on aquifer connectivity at the regional scale and were thus not considered in the process of the classification.

Distribution Analyses of Hydrogeochemical Species (including As):

For the depth distribution analyses, we have classified the delta aquifers into three depth zones, i.e., depths ≤60 m below MSL are classified as shallow; >60–150 m below MSL as intermediate; and >150–300 m below MSL as deep. These depth-class thresholds were selected based on the maximum depth of abstraction for the different types of pumping wells within the delta, i.e., the majority of the shallow hand-pumped tube wells and motorized irrigation wells tap aquifer depths down to ~60 m, whereas the underlying aquifers to a depth of ~150 m are mostly tapped by the deeper hand-pumped (India Mark II/III) wells, and the aquifers below this depth remain less exploited. Based on this, about 77% of the As measurements were obtained from wells tapping the shallow aquifers, whereas ~16% of the measured wells tap the intermediate-depth aquifers and ~7% of the wells exploit the deep delta aquifers. Among the wells sampled during the field survey by Chakraborty et al. (in review), ~33% tap shallow aquifers, while ~35% and ~26% tap the intermediate and deeper aquifers, respectively. The remaining wells are deeper than 300 m below MSL (the maximum depth of our lithologic model) and were thus excluded from this study. Solute concentrations in groundwater below the minimum detection limit were assigned a value half of the detection limit to minimize error (Ayotte et al., 2012).

SI Table 1: Details of borehole litholog data used for the lithological model

Borehole Litholog Data		
Source	**Area of collection**	**Counts**
Public Health Engineering Department (PHED), West Bengal (India) [http://maps.wbphed.gov.in/web_gis]	India	1049
Aquifer Database Inventory, Department of Health and Engineering (DPHE), Bangladesh [http://dphe.gov.bd/aquifer/index.php]	Bangladesh	1598
Bangladesh Water Development Board (BWDB), Bangladesh (BWDB, 2013a)	Bangladesh	465

SI Table 2: Details of groundwater arsenic data

Groundwater Arsenic Data			
Source	**Area of collection**	**Year of collection**	**Counts**
United Nations Children's Fund (UNICEF) and Public Health Engineering Department (PHED), West Bengal Joint Plan of Action (JPOA) PHED, (2006)	India	2003-2006	97,714
British Geological Survey (BGS) and the Department of Health and Engineering (DPHE), Bangladesh [BGS and DPHE, 2001] [https://www.bgs.ac.uk/research/groundwater/health/arsenic/Bangladesh/data.html]	Bangladesh	1998-1999	1,059
Bangladesh Department of Health and Engineering (DPHE) Bangladesh Water Development Board (BWDB) Climate Change Trust Fund Project (BWDB, 2013b)	Bangladesh	1995-2005 2011-2013	1,586

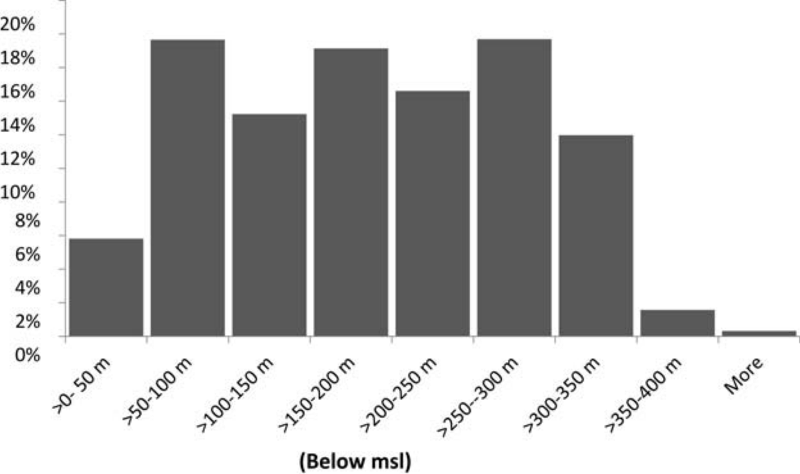

SI Figure 1:The depth distribution of the borehole lithologs used for the lithological model

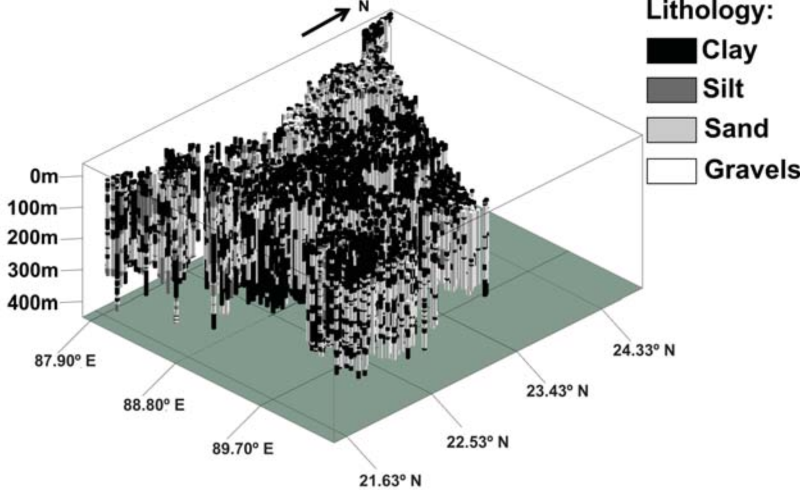

SI Figure 2: Distribution of the borehole lithologs in a three dimensional geospatial framework

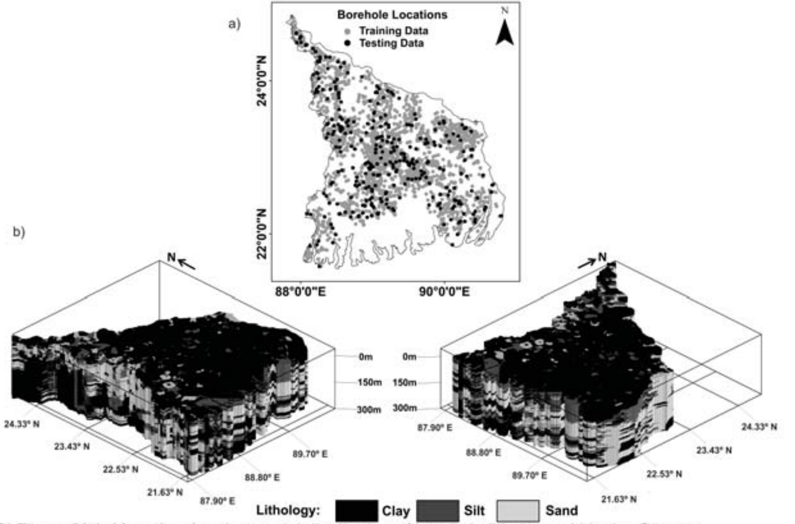

SI Figure 3(a): Map showing the spatial distribution of borehole lithologs within the Ganges River delta; (b) lithologic model of the Ganges River delta subsurface (to a depth of 300 m below MSL), viewed from southwest and southeast.

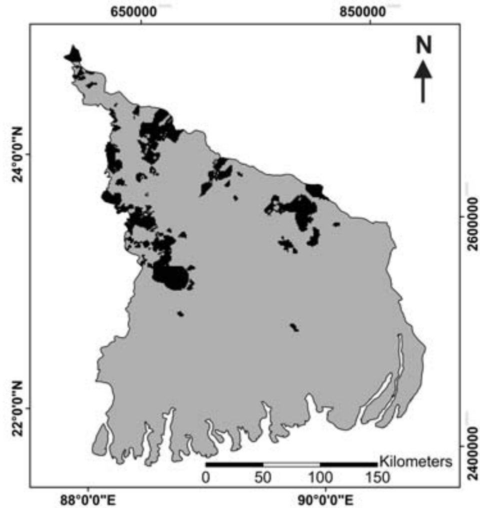

SI Figure 4: Plan view of the spatial disposition of gravel layers within the Ganges River delta subsurface (up to a depth of 300 m below msl)

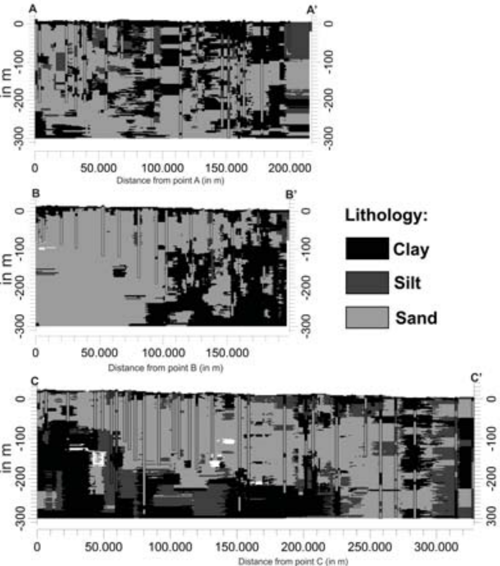

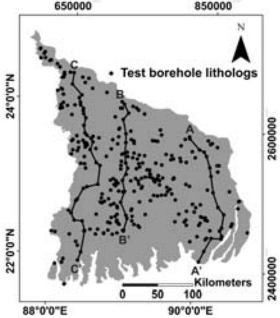

SI Figure 5: Model validation (first step), showing 62 test boreholes overlaid on the predicted lithological framework of the Ganges River delta subsurface along 3 sections that passes through these boreholes

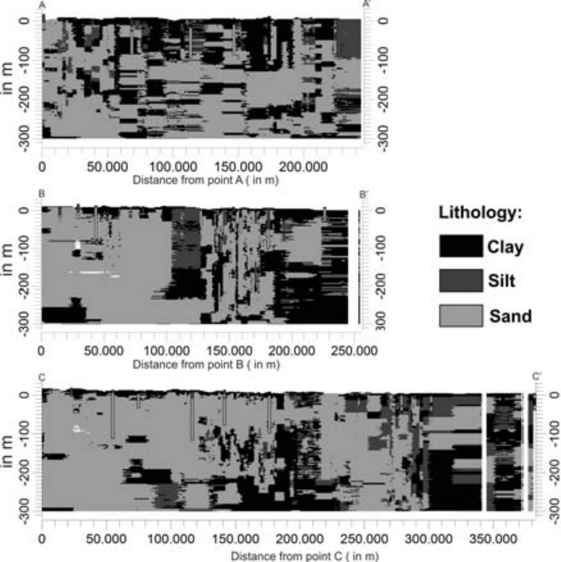

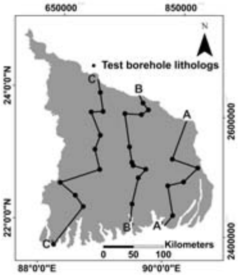

SI Figure 6: Model validation (second step), showing 25 boreholes [compiled from Umitsu (1987), Goodbred and Kuehl (2000), and Goodbred et al. (2014)] overlaid on the predicted lithological framework of the Ganges River delta subsurface along 3 cross-sections that pass through these boreholes

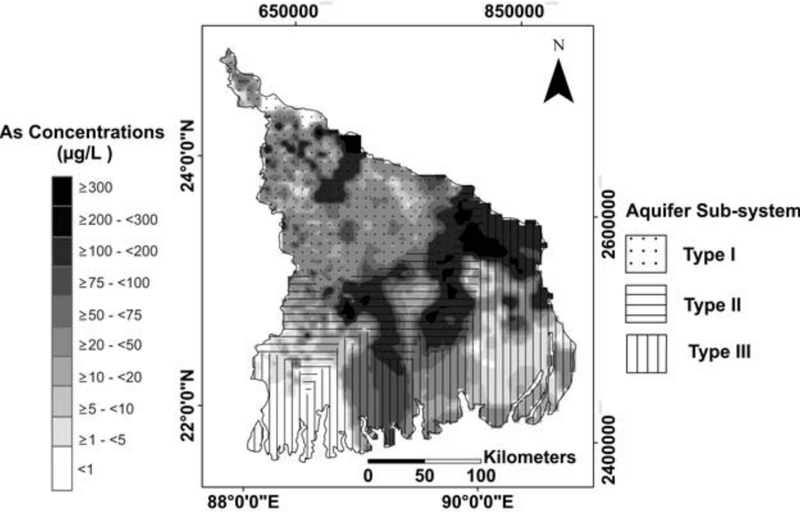

SI Figure 7: Map showing the distribution of groundwater arsenic concentration within the Ganges River delta, developed using kriging

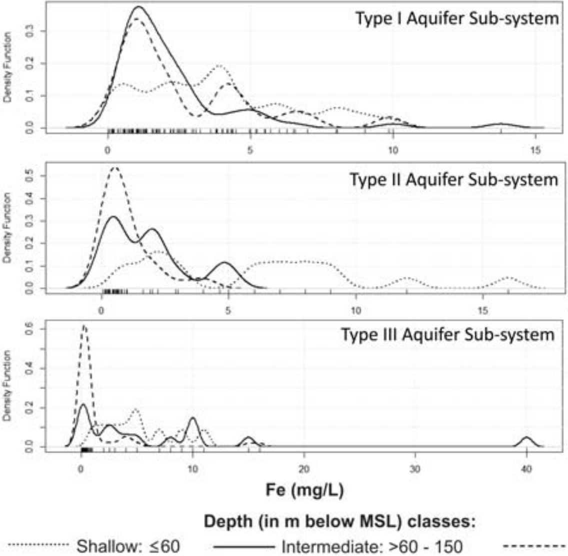

SI Figure 8: Kernel density (bandwidth=0.5) plots showing the distribution of dissolved Fe among the major aquifer sub-systems of the delta

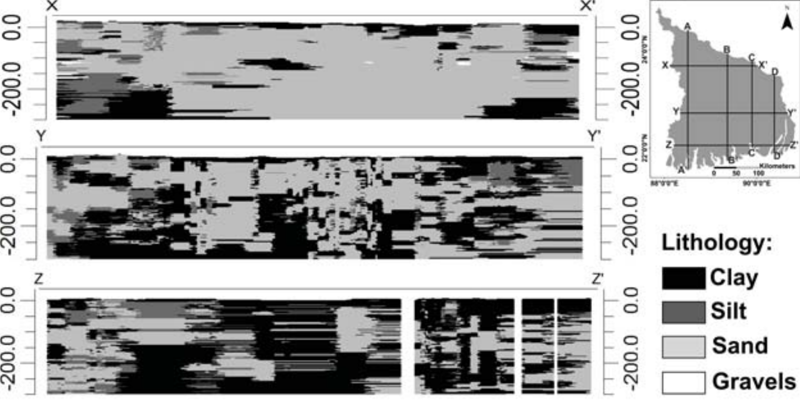

SI Figure 9: 2-dimensional modeled lithological sections (to a depth of 300 m below msl) along four north-south and three east-west directions across the Ganges River delta

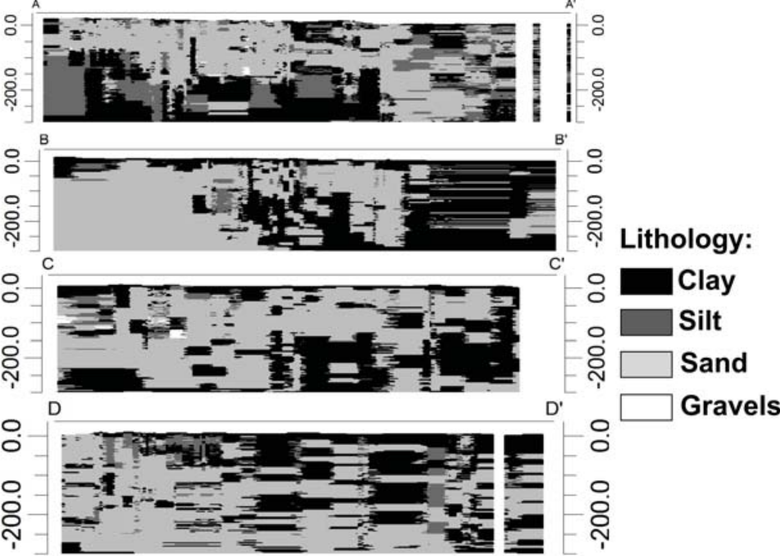

SI Figure 9(cont.) : 2-dimensional modeled lithological sections (to a depth of 300 m below msl) along four north-south and three east-west directions across the Ganges River delta

References:

Ayotte, J.D., Cahillane, M., Hayes, L., and Robinson, K.W., 2012, Estimated Probability of Arsenic in Groundwater from Bedrock Aquifers in New Hampshire, 2011: U.S. Geological Survey Scientific Investigations Report 5156, 25 p., https://doi.org/10.3133/sir20125156.

Bangladesh Water Development Board (BWDB), 2013a, Hydrogeological Study and Mathematical Modelling to Identify Sites for Installation of Observation Well Nest. Water Quality Volume 2: Dhaka, Bangladesh, Bangladesh Water Development Board (BWDB) and Institute of Water Modelling (IWM).

Bangladesh Water Development Board (BWDB), 2013b, Hydrogeological Study and Mathematical Modelling to Identify Sites for Installation of Observation Well Nest. Water Quality Volume 5: Dhaka, Bangladesh, Bangladesh Water Development Board (BWDB) and Institute of Water Modelling (IWM).

Chakraborty, M., Mukherjee, A., Ahmed, K.M. Regional-scale Hydrogeochemical Evolution across the arsenic-enriched transboundary aquifers of the Ganges River Delta system, India and Bangladesh. STOTEN [In Revision].

Goodbred, S.L., and Kuehl, S.A., 2000, The significance of large sediment supply, active tectonism, and eustasy on margin sequence development: Late Quaternary stratigraphy and evolution of the Ganges–Brahmaputra delta: Sedimentary Geology, v. 133, p. 227–248, https://doi.org/10.1016/S0037-0738(00)00041-5.

Goodbred, S.L., Paolo, P.M., Ullah, M.S., Pate, R.D., Khan, S.R., Kuehl, S.A., and Rahaman, W., 2014, Piecing together the Ganges–Brahmaputra–Meghna River delta: Use of sediment provenance to reconstruct the history and interaction of multiple fluvial systems during Holocene delta evolution: Geological Society of America Bulletin, v. 126, no. 11□12, p. 1495–1510, https://doi.org/10.1130/B30965.1.

Michael, H.A., and Voss, C.I., 2009, Control on groundwater flow in the Bengal Basin of India and Bangladesh: Regional modeling analysis: Hydrogeology Journal, v. 17, p. 1561–1577, https://doi.org/10.1007/s10040-008-0429-4.

Public Health Engineering Department (PHED), 2006, Results of Tubewells Tested for Arsenic under UNICEF Supported JPOA for Arsenic Mitigation.

Umitsu, M., 1987, Late Quaternary sedimentary environment and landform evolution in the Bengal lowland: Geographical Review of Japan, ser. B, v. 60, p. 164–178, https://doi.org/10.4157/grj1984b.60.164.